MSA UNIVERSITY ENGINEERING JOURNAL

The Structural Behavior of Ferrocement Lightweight Walls

Abeer M. Erfan[1, a], Yousry B. Shaheen[2, b], Ragab M. Abd Elnaby[3, a], Khaled A. SadAllah[4, a]

[a] Department of Structural Engineering, Shoubra Faculty of Engineering, Benha University, 108 Shoubra street, Shoubra, Cairo, Egypt
[b] Department of Civil Engineering, Faculty of Engineering, Menoufia University, Egypt
E-mail: [a]abir.arfan@feng.bu.edu.eg, [b] ybishaheen@gmail.com, [a] ragab.migahed@gmail.com, [a] khaled.abdelnasser17@gmail.com

Abstract

Experimental and theoretical study on the structural behaviour of ferrocement lightweight walls subjected to distributed compressive loads is presented in this investigation. Casting and testing nine walls with overall dimensions of 100 x500x1000mm, divided into four groups with longitudinal reinforcement of 10Φ10 bars, was part of the experimental procedure. All groups contained four lightweight bricks with dimensions of 40x200x400 mm length, aligned along the specimen with interspaces between each brick. Ultimate loads, modes of failure, first crack loads, service. Loads, and ductility ratios were studied in relation to the characteristics of steel reinforcing type, namely welded and expanded wire meshes. In the theoretical study, NLFEA model using ANSYS R19 program was used to be compared with the experimental results which showed a good agreement with experimental program with approximately ratio of 88 %. The lightweight ferrocement walls in Groups II, III and IV that reinforced with welded and expanded wire meshes have showed enhancement ratios in all mechanical properties with respect to Control Group I with no meshes and using expanded wire mesh showed higher ratios of enhancement with respect to welded wire mesh. It is interesting to note that combining welded and expanded steel wire meshes showed superior mechanical properties.

Keywords: Ferrocement; Lightweight walls; Cracking; Ductility; Finite element method; Steel Meshes; Expanded steel mesh; Welded steel mesh.

1. Introduction

Ferrocement is a building material that has demonstrated excellent fracture control, impact resistance, and toughness, due to its tight spacing and uniform distribution of reinforcement inside the material. Many researchers have reported on the material's physical and mechanical properties, and there are a variety of test data to define its design and construction performance criteria. Recently, ferrocement has proved to be a viable option for the use as a material in low-income residential buildings in developing countries [1-3].

Ferrocement is a concrete mortar matrix with metal mesh reinforcement. Ferrocement is defined by its steel mesh surface area, volume ratio, concrete surface cover, and mortar quality. Ferrocement was the first type of reinforced concrete to be developed. Ferrocement performs as reinforced concrete, except that the proper distribution of reinforcement over the mortar reduces the development of cracks. Ferrocement has several applications because of its unique mechanical properties such as improving strength, service. Loads, energy absorption and its lightweight make it a good alternative to conventional reinforcement [4-5].

Shaheen et al. suggest ferrocement panels could be load-bearing wall components. Panels proposed weigh less than standard ones. Thin layers of ferrocement were reinforced with welded steel mesh and expanded steel mesh. Lightweight brick formed the panel's core. Shear connections linked each layer's steel meshes. Steel mesh reinforcement produced the ferrocement surface layer ten millimetres thick; and the thickness of two layers was 15 mm. Experiments were conducted on the suggested panels. Ten sandwich panels. 600mm x 700mm tested until failure. Each panel's displacement and cracking were investigated. The suggested panels provide large energy absorption, ductility, fracture resistance, ultimate and serviceability loads [6].

E. H. Fahmy et al. studied employing precast, permanently shaped reinforced mortar forms filled with different core materials as an alternative to the conventional reinforced concrete beam. They combined theory and experiment. Thirty U-shaped reinforced mortar beams were cast and tested. They cast three equal-sized control beams. Permanent U-shaped forms were reinforced with weld mesh and X8 expanded steel mesh. Conventional concrete, lightweight concrete brick, and recycled concrete were studied. Connecting core material and precast permanently reinforced mortar form, utilize adhesive bonding and mechanical shear connections. Three 1,800-mm test specimens were tested as beams. Permanently formed vs. unshaped beams were compared. The suggested beams improved crack resistance, serviceability, ultimate strength, and energy absorption. Theoretical and experiment agreed well [7].

After these studies the presented study presents the effect of using lightweight ferrocement concrete in the behavior of walls under compressive distributed load.

2. Experimental Program

The experimental program consisted of four groups of 100 mm width, 500 mm length and 1000 mm height walls. Group I have the control specimen which has longitudinal reinforcement of 10 Φ 10 and closed transverse reinforcement of 12 Φ 8. Group II has four specimens which have longitudinal reinforcement of 10 Φ 10 and closed transverse reinforcement of 5 Φ 8 and have One, Two, Three and Four layers of steel welded steel mesh respectively. Group III includes three specimens having the same reinforcement of group II and have One, Two and Three layers of steel expanded steel mesh. Group IV has one specimen which has the same reinforcement of group II and Group III and includes 2 layers of welded steel mesh and one layer of expanded steel mesh. All Groups include four lightweight bricks having dimensions of 40 mm thickness, 400 mm width and 200 mm length aligned along the specimen having interspaces between each brick. It is important to note that the experimental program was executed in the American University in Cairo, Egypt laboratory.

2.1. Characteristics of Materials

After 28 days, a compressive strength of 45 MPa could be achieved using the concrete mixture utilized in the experimental program, the components of which are listed in Table 1. Steel with a yield strength of 360 MPa was utilized. Expanded and welded steel meshes were both employed to produce composite layers, the details of which are presented in Table 2 and shown in Fig. 1.

Table 1: Concrete Mixes, Materials Weight.

Materials	**Mix Component** $\mathbf{F_{cu} = 45\ MP_a}$
Cement	477.74 Kg/m^3
Silica Fume	68.25 Kg/m^3
Fly Ash	136.5 Kg/m^3
Fine Aggregates	1364.99 Kg/m^3
Water	238.87 Kg/m^3
Polypropylene Fibers	1.35 Kg/m^3
Super Plasticizer	13.65 Kg/m^3

Table 2: Steel Meshes Mechanical Properties.

Mesh type	Tensile strength (MPa)	Young's modulus (GPa)	Opens dimensions (mm)	Diameter (mm)
welded steel mesh	400	170	10.0x10.0	0.7
Expanded steel mesh	250	120	31.0x16.5	1.25

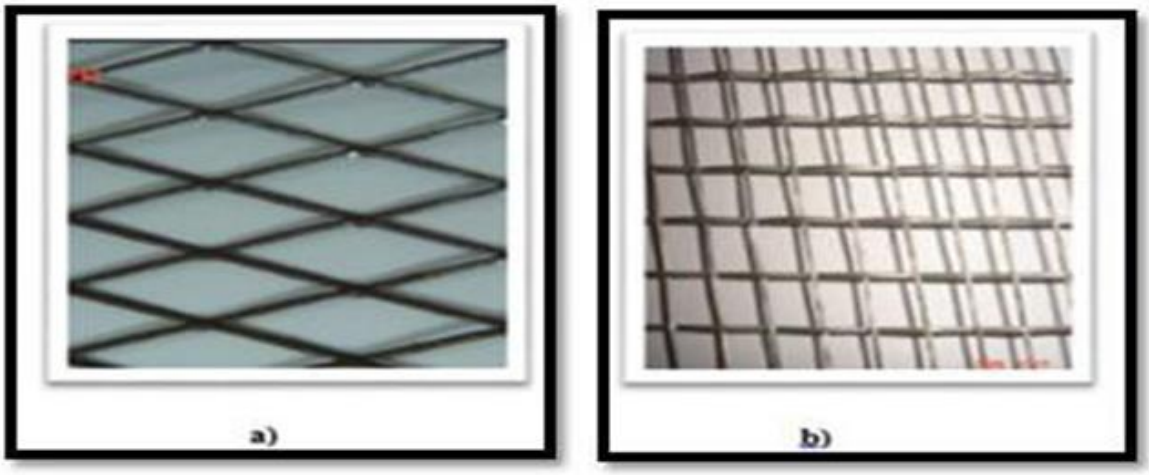

Figure 1: Steel Meshes; A) Expanded Steel. B) Welded Steel.

2.2. Experimental Walls Description

The experimental program consists of four groups of specimens. Group I contain the control specimen (W1) which have longitudinal reinforcement 10 Φ 10, transverse reinforcement 12 Φ 8 and have 4 lightweight bricks. The control specimen also doesn't have any steel mesh layers. The other three groups have the same longitudinal reinforcement, 5 Φ 8 of transverse reinforcement and the same number of lightweight bricks. Group II includes (W2, W3, W4, and W5) walls which have included welded steel mesh reinforcement, the number of layers for each specimen are one, two, three and four layers respectively. Group III consists of (W6, W7 and W8) walls that have included expanded steel mesh, the number of layers for each specimen are one, two and three layers respectively. Group IV which only has (W9) which consists of two layers of welded steel meshes and one layer of expanded steel mesh. All Groups reinforcement details are described in Table 3 and all walls geometric and reinforcement details are shown in Fig. 2. All specimens' photos before casting are shown in Fig.3.

Table 3: Specimens Descriptions and Notations.

Groups	Specimen ID.	Description of specimens	Reinforcement		LightWeight Bricks (LWB) (40*400*200 mm)
			Longitudinal	Transverse	
Group I	W 1	Control specimen	10 Φ 10	12 Φ 8	Four Bricks
Group II	W 2	One layer welded wire mesh	10 Φ 10	5 Φ 8	Four Bricks
	W 3	Two layers welded wire mesh	10 Φ 10	5 Φ 8	Four Bricks
	W 4	Three layers welded wire mesh	10 Φ 10	5 Φ 8	Four Bricks
	W 5	Four layers welded wire mesh	10 Φ 10	5 Φ 8	Four Bricks
Group III	W 6	One layer expanded wire mesh	10 Φ 10	5 Φ 8	Four Bricks
	W 7	Two layers expanded wire mesh	10 Φ 10	5 Φ 8	Four Bricks
	W 8	Three layers expanded wire mesh	10 Φ 10	5 Φ 8	Four Bricks
Group IV	W 9	Two layers welded wire mesh + One layer expanded wire mesh	10 Φ 10	5 Φ 8	Four Bricks

2.3. Test Setup

The tested walls sections were tested under a distributed compressive load testing machine with a maximum capacity of 5000 KN as shown in Fig.4. Three LVDT gauges were used with high accuracy to measure the vertical and horizontal displacements as shown in Fig.4. Two Baio (Pi) gauges were also used to observe strains and crack width along the walls. The load was kept increasing until the failure load and maximum displacements were reached.

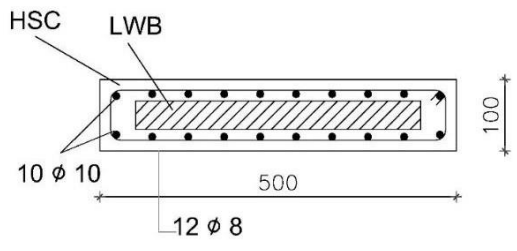

a) W 1 - Control

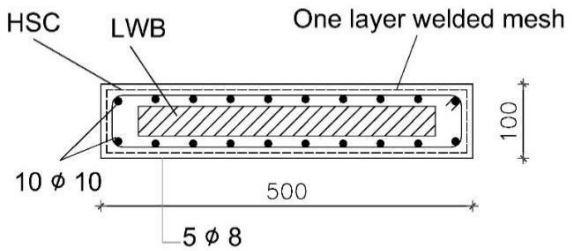

b) W 2

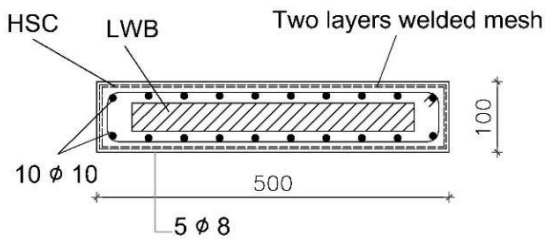

c) W 3

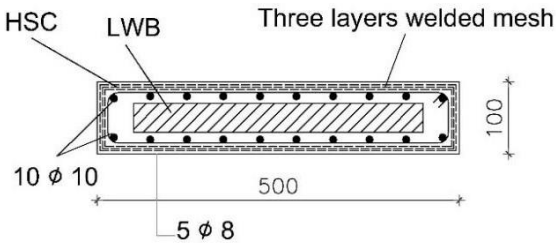

d) W 4

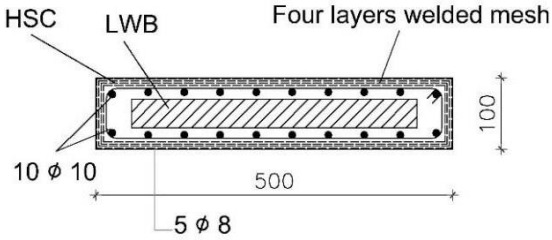

e) W 5

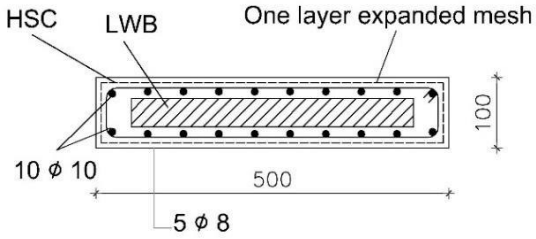

f) W 6

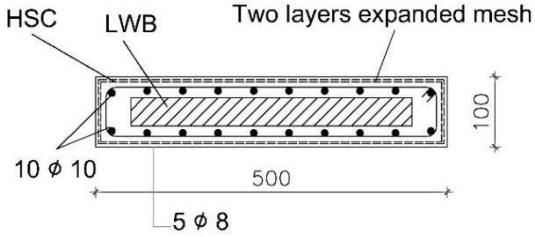

g) W 7

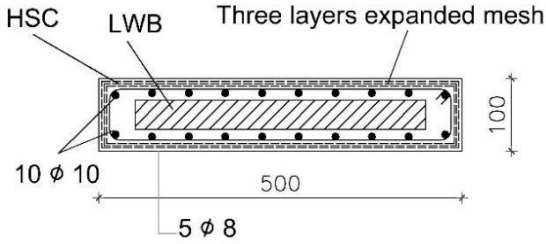

h) W 8

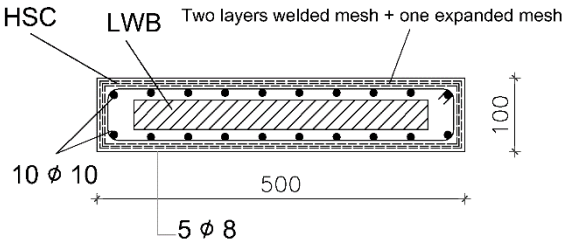

i) W 9

Figure 2: Walls Geometric Shape and Reinforcement Details

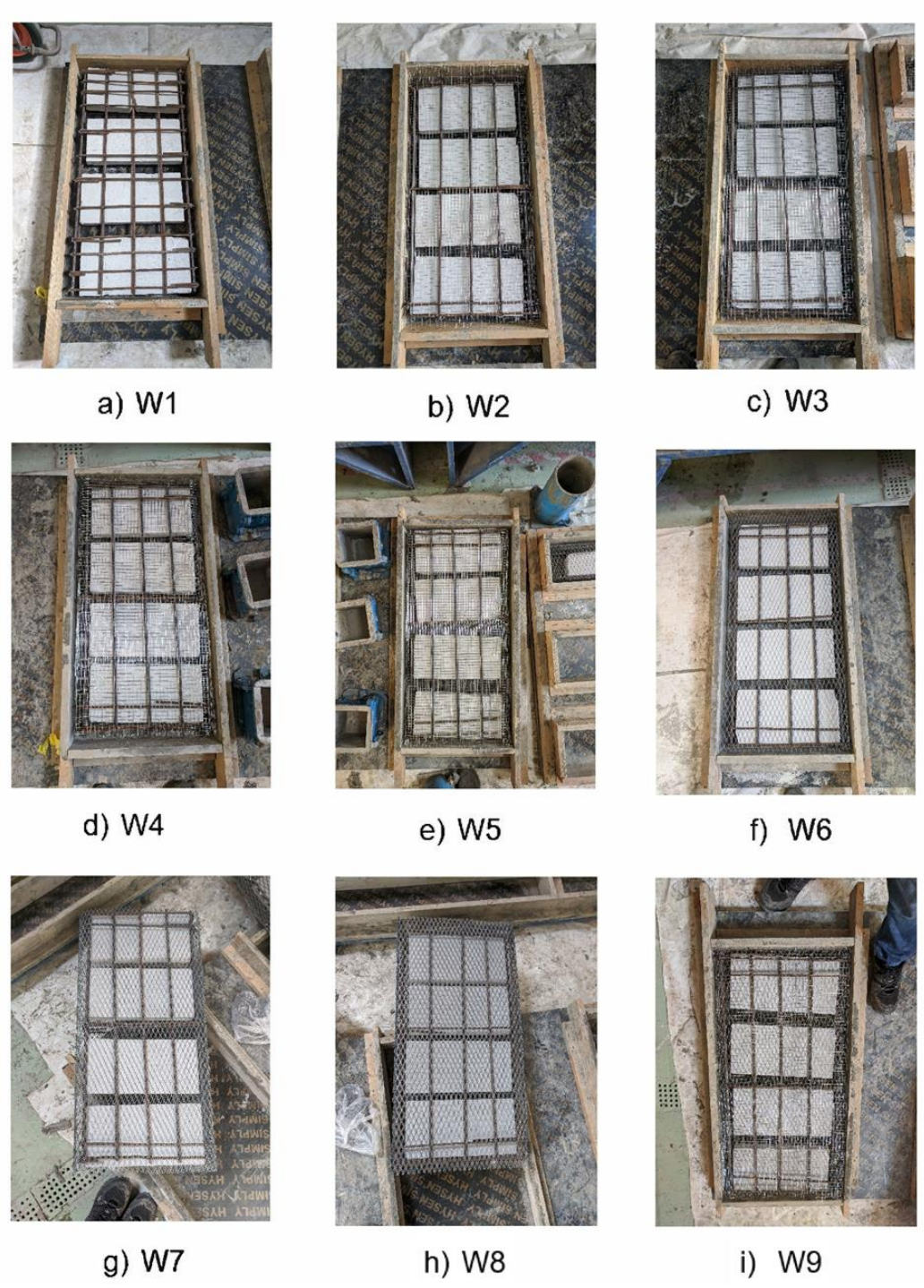

Figure 3: Walls Photos Before Casting.

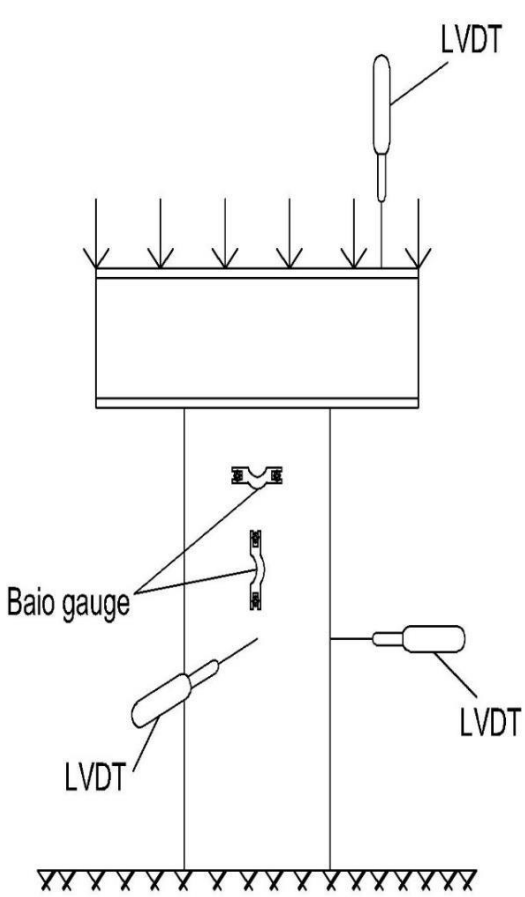

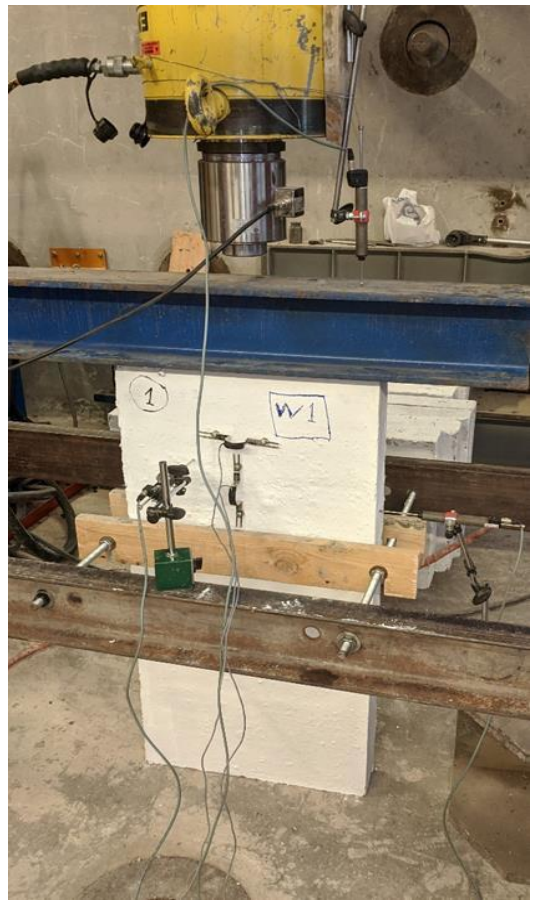

A) **B)**

Figure 4: Test Setup; A) Schematic Shape. B) Photo of The Test Setup

3. Experimental Results and Discussions

The experimental results of the distributed compressive loading of the tested walls were observed and summarized in Table 4. Ultimate failure loads, stress, first crack and service. Loads, ductility ratios, and energy absorption attributes were all determined and recorded for each of the tested walls. Load-horizontal displacement curves and load-vertical displacement curves for all the tested walls are shown in Fig.5 and 6 respectively.

Table 4: All Specimens Experimental Results.

Groups	Specimen ID.	F.C.L KN	Ultimate Load stress KN	N/mm2	Service Load KN	Def. at F.C.L mm	Max. Defl mm	Duct. ratio	Energy Absorp. KN.mm
Group I	W 1	425.64	655.87	13.12	409.26	0.53	2.57	4.88	1537.63
Group II	W 2	428.48	668.24	13.36	416.99	0.34	1.68	4.87	1024.32
	W 3	430.65	676.40	13.53	422.09	0.42	2.08	4.91	1283.69
	W 4	432.22	681.16	13.62	425.07	0.44	2.14	4.93	1331.79
	W 5	451.44	717.87	14.36	448.01	0.54	2.68	4.97	1753.08
Group III	W 6	430.58	674.36	13.49	420.82	0.38	1.88	4.90	1153.68
	W 7	434.21	685.91	13.72	428.04	0.48	2.35	4.94	1468.64
	W 8	470.56	766.13	15.32	478.18	0.54	2.75	5.09	1922.34
Group IV	W 9	436.39	690.67	13.81	431.01	0.51	2.52	4.95	1589.25

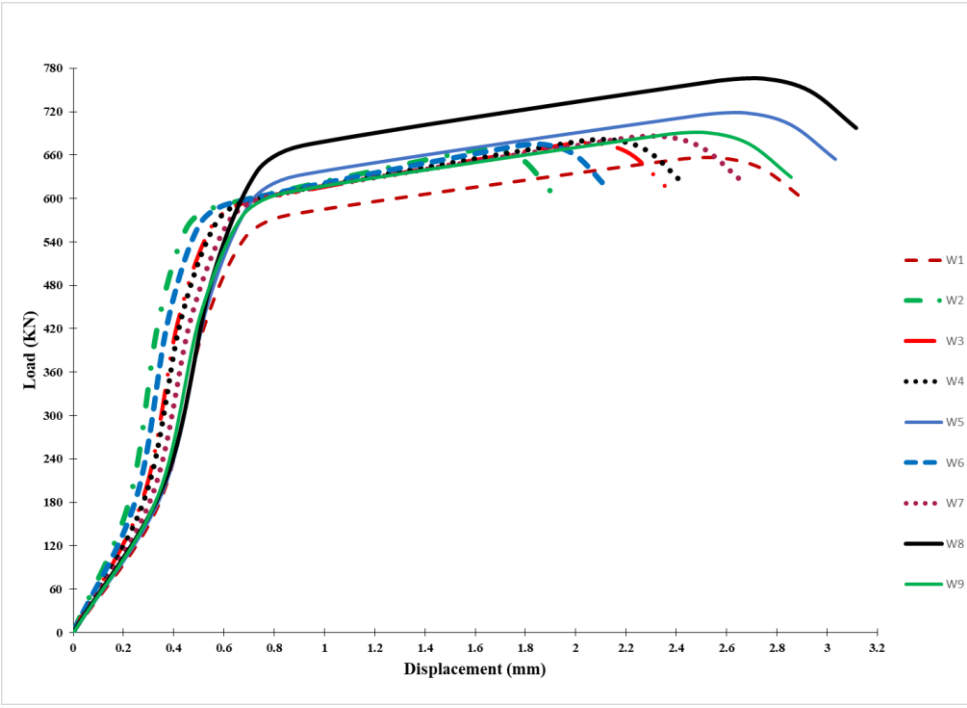

Figure 5: Load - Horizontal Displacement Curves for All Specimens.

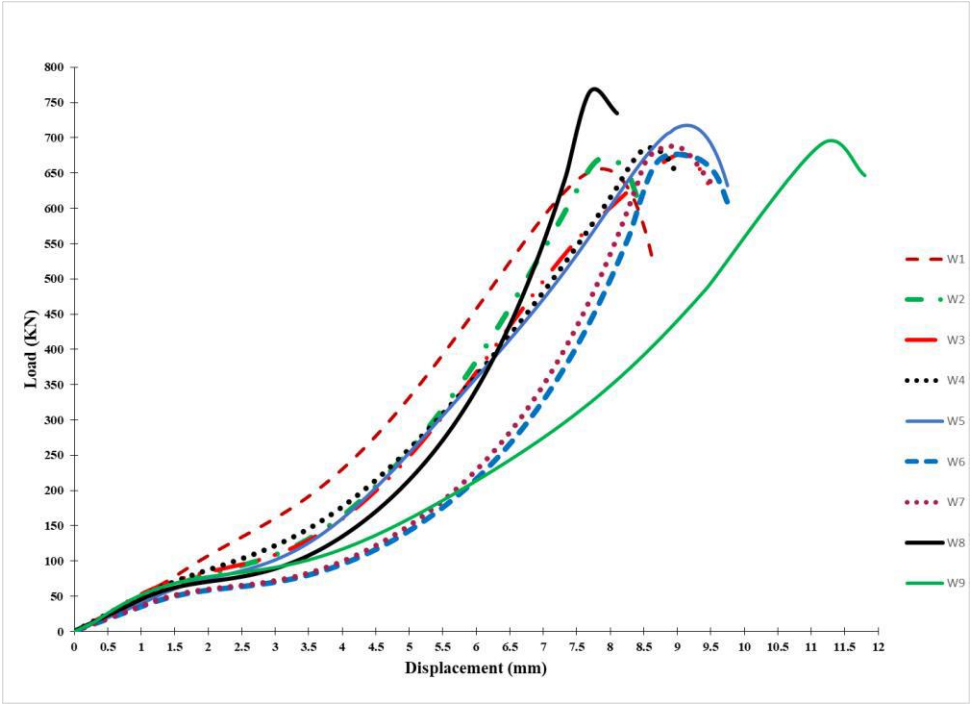

Figure 6: Load - Vertical Displacement Curves for All Specimens.

3.1. Ultimate Experimental Failure and First Crack Load

The experimental program consists of four groups group I consists of the control specimen W1 has a first crack load of 425.64 KN and has ultimate load of 655.87 KN. Group II which consists of specimens W2, W3, W4 and W5 that were reinforced with welded steel meshes have enhancement in first crack load by 0.67%, 1.18%, 1.55% and 6.06% respectively and the enhancement in the ultimate failure load were 1.89%, 3.13%, 3.86% and 9.45% respectively. Group III which consists of specimens W6, W7 and W8 that were reinforced with expanded steel meshes have enhancement in first crack load by 1.16%, 2.01% and 10.55% respectively and the enhancement in the ultimate failure load were 2.82%, 4.58% and 16.81% respectively. Group IV which consists of specimen W9 that were reinforced with both welded and expanded steel meshes have enhancement in first crack load by 2.53% and the enhancement in the ultimate failure load was 5.31%.

It's interesting to note that the increase in the numbers of steel layers meshes expanded or welded have a positive influence on the first and ultimate failure loads of the specimens and combining welded and expanded steel meshes as in group IV specimen has a good enhancement first crack load, crack distribution and ultimate failure load. A comparison between the four groups specimens' ultimate and first crack loads are shown in Fig.7.

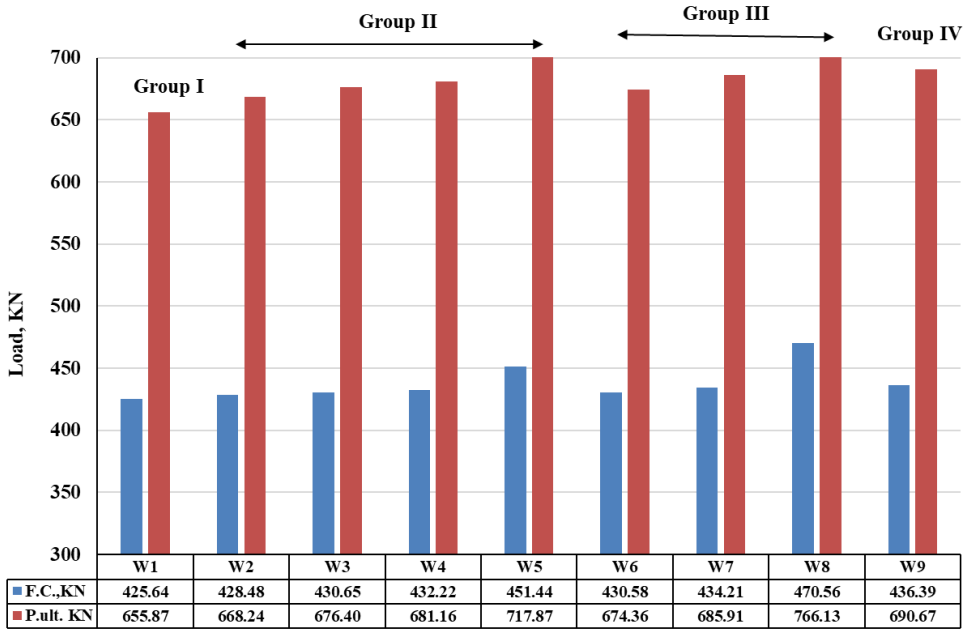

	W1	W2	W3	W4	W5	W6	W7	W8	W9
F.C.,KN	425.64	428.48	430.65	432.22	451.44	430.58	434.21	470.56	436.39
P.ult. KN	655.87	668.24	676.40	681.16	717.87	674.36	685.91	766.13	690.67

Figure 7: Comparison of Ultimate and First Crack Load Between All Groups.

3.2. Cracking behavior

The first crack load, the ultimate failure load, the reinforcement yield stress and the reinforcement's particular surface area are all important factors in determining the crack width. According to the observations of the tested walls, steel mesh reinforcement is significantly more effective than conventional reinforcement for limiting crack width. The failure of the specimen did not cause any spalling in the concrete mortar cover was a positive behavior. Initial cracks appeared on the specimens' edges as the loading increased till failure. Cracks progressed vertically and additional flexural cracks formed when the strain of the specimen was increased. The cracks in the specimens occurred diagonally as the applied force became closer to the point of failure. A big, diagonal fissure appeared at the specimen's end as it failed. In comparison to the control specimen, the number of developed cracks along the other specimens was decreased. It was clear that the use of wire steel reinforcement had decreased the cracks numbers and also decreased the cracks width. All the cracking patterns for the lightweight walls under compression loads are shown in Fig.8

a) W1 b) W2 c) W3

d) W4 e) W5 f) W6

g) W7 h) W8 i) W9

Figure 8: Tested Walls Crack Patterns.

3.3. Ductility Ratio

The definition of the ductility ratio is the ratio between out of plain horizontal displacement of tested wall at ultimate failure load to that at first crack load. The walls reinforced with welded meshes in Group II showed higher ductility ratio than the control specimen except for specimen W2. The ratios of enhancement were 0.55%, 0.89% and 1.80% for W3, W4 and W5 respectively while W2 showed decreasing in ductility ration by -0.16%. Group III specimens with expanded meshes reinforcement showed improvement of ratios by 0.26%, 1.12%, 4.22% for W6, W7 and W8 respectively and the mixed reinforced specimen w9 show improvement by 1.32% with respect to the control specimen. A comparison between the four groups' specimens' ductility ratios are shown in Fig.9 which shows that W8 has the highest enhancement ratio.

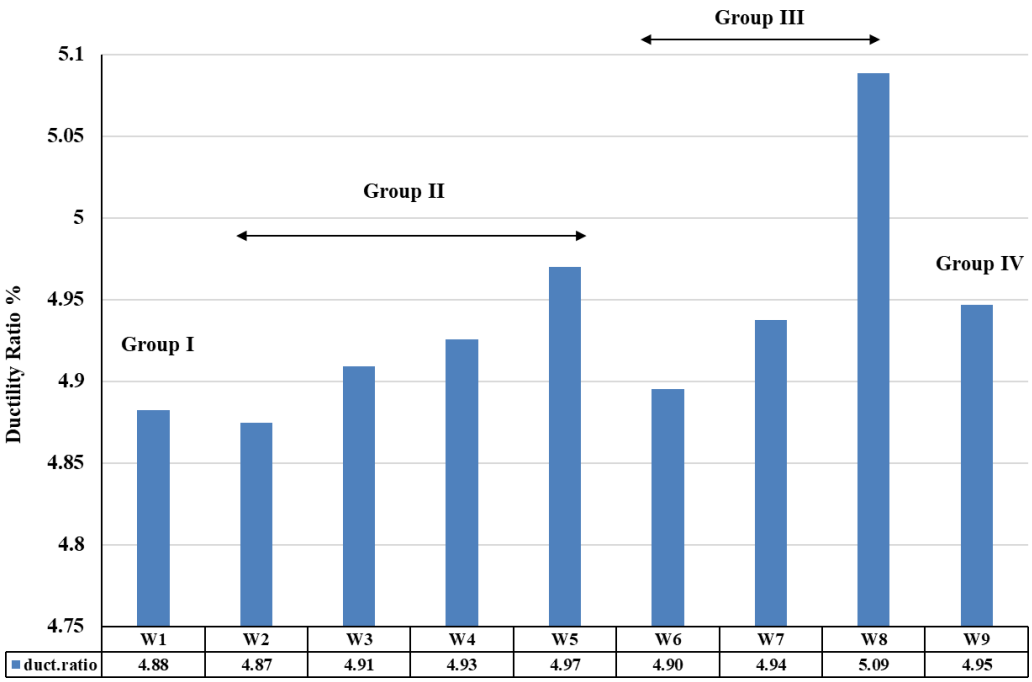

Figure 9: Ductility Ratios % Comparison.

3.4. Energy Absorption

Each wall's energy absorption was determined by determining the area below its respective load displacement curve. The absence of stirrups in Group II and Group III even with the presence of steel mesh layers has a negative effect on energy absorption for the specimens except for W5 and W8. The increase in steel mesh layers as in W5, W8 and W9 have an enhancement in energy absorption by 14.01%, 25.02% and 3.36% respectively with respect to control specimen with stirrups (W1). The increase in energy absorption of steel mesh reinforced specimens enhances their dynamic behavior. There were sharp differences between the tested walls in terms of energy absorption, which are shown in Fig. 10.

3.5. Serviceability Load

In order to determine the service load, the following formula was used: (Experimental ultimate failure load - 1.4 own weight) then divide the results by 1.6 [6]. Group II showed enhancement in service. Load by 1.89%, 3.13%, 3.86% and 9.47% for W2, W3, W4 and W5 respectively with respect to the control specimen. Improvement ratios of W6, W7 and W8 of group III are 2.82%, 4.59% and 16.84% respectively while w9 showed 5.31% enhancement ratio with respect to the control specimen W1. Fig.11 highlights the contrast in the service loads of the tested walls.

3.6. Horizontal Displacement of Tested Walls

The out of plain horizontal displacement was detected using LVDT placed against the out of plain side of the tested walls. Displacements at first crack load and ultimate failure load are shown previously for all specimens in table 4. It's necessary to note that using the steel meshes has decreased the displacement as in W2, W3, W4, W6, W7 and W9 but the increase of the ultimate failure load due to increasing the number of used meshes layers has increased the displacement in W5 and W8. Displacement comparisons of the tested walls are shown in Fig.12.

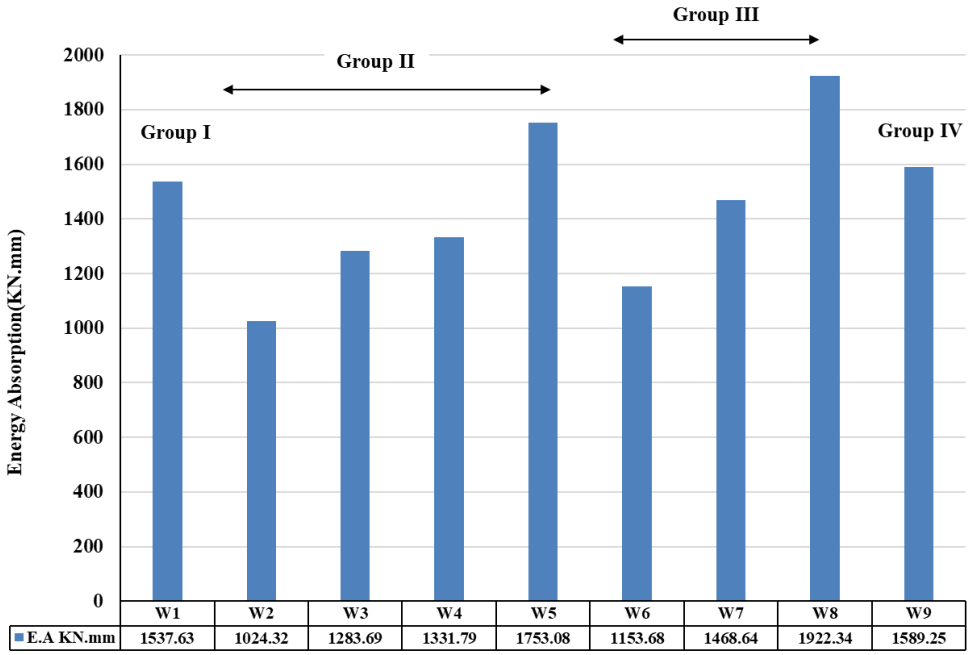

Figure 10: Energy Absorptions Comparison.

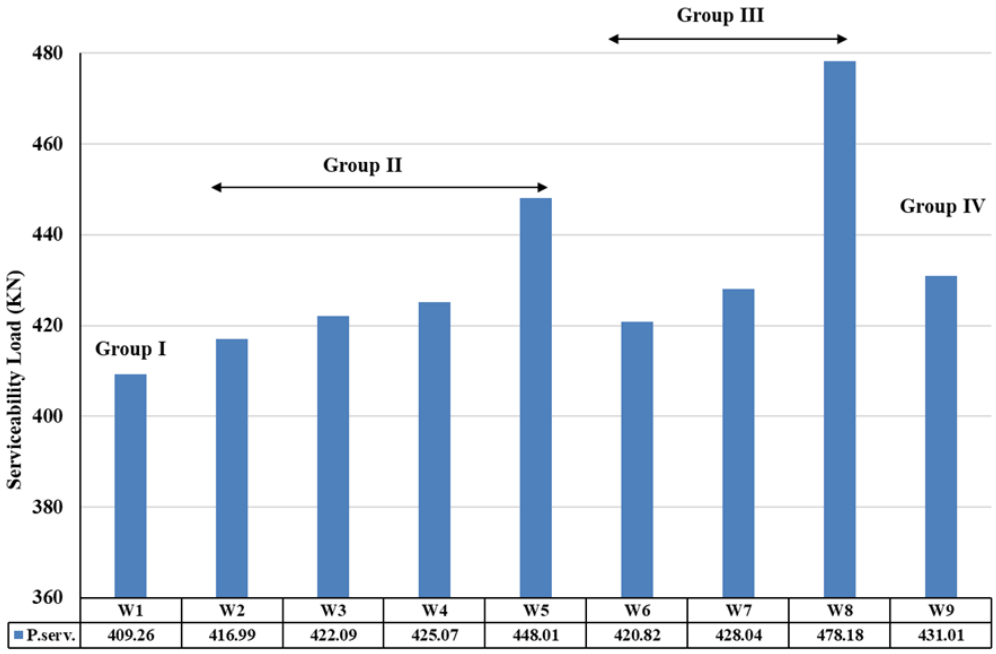

Figure 11: Serviceability Loads Comparison.

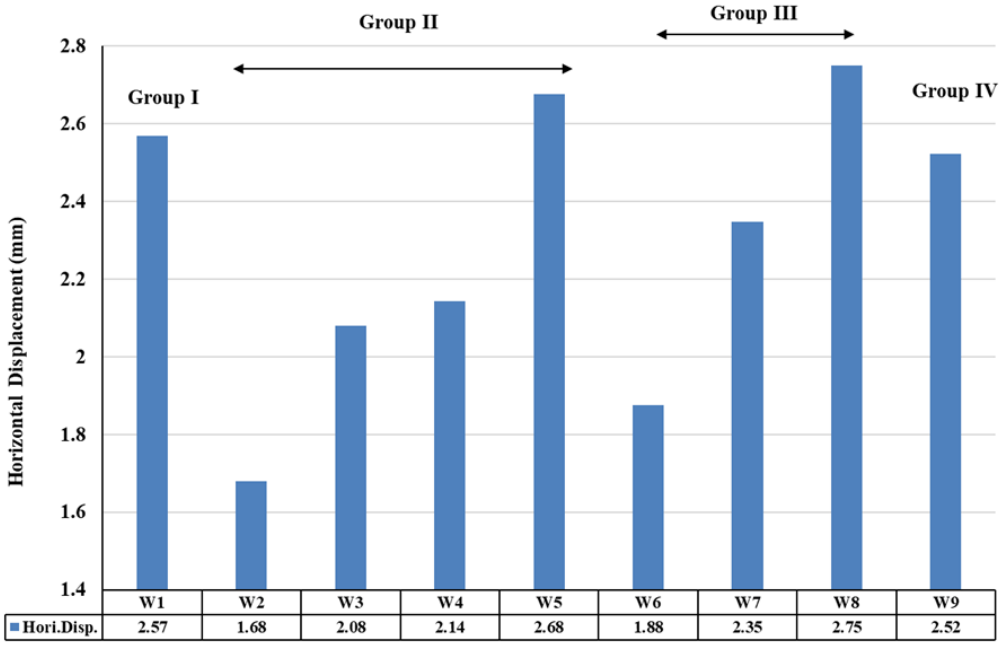

Figure 12: Horizontal Displacements Comparison.

4. Non-Linear Finite Element Analysis

Non-linear finite element analysis (NLFEA) was used to verify experimental results and gain insight into the structural performance of a ferrocement lightweight wall reinforced with varied steel meshes and exposed to distributed compressive loads. Results obtained from NLFEA were discussed as ultimate failure and first crack loads and crack patterns.

4.1 Non-Linear Finite Element Walls Modelling

ANSYS2019-R1 was used for the non-linear finite element modelling. Results from testing were used to define the finite element model. A failure mode estimate could be generated with the use of this type of study, which is carried out by performing a complete three-dimensional nonlinear finite element analysis of the experimental setup. In this study, concrete and steel meshes were defined using SOLID65 element, LINK180 3-D element was used to represent reinforcement bars and SOLID185 was used to represent loading plate and support. The different steel meshes were represented by calculating their volumetric ratio in concrete element. The volumetric ratio of one, two and three layers of expanded steel meshes was 0.00349, 0.00698 and 0.01047 respectively and the volumetric ratio of one, two, three and four layers of welded steel meshes was 0.000418, 0.000836, 0.001254 and 0.001672 respectively while two layers of welded steel meshes combined with one layer of expanded steel mesh were represented using the previous volumetric ratios. The established geometrical model in Figure 13 is identical to the tested specimens as discussed above.

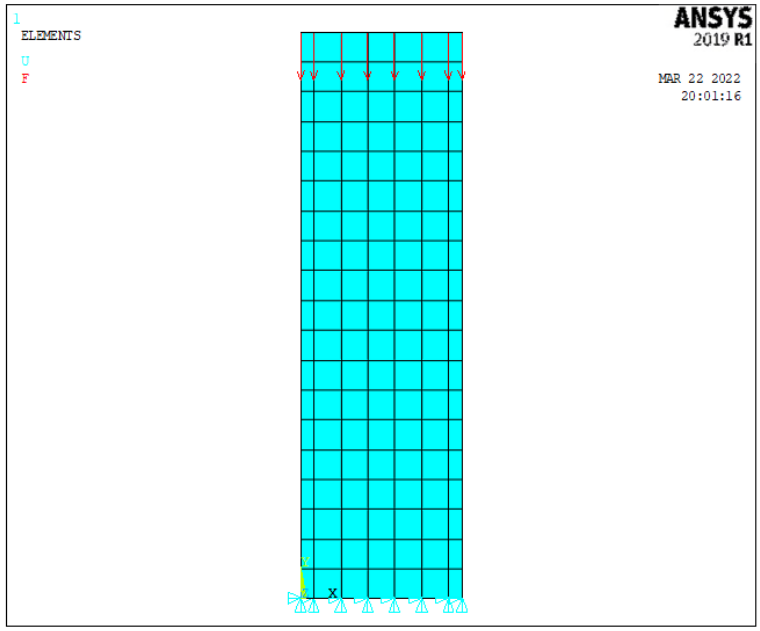

Figure 13: Simulated Specimens' Geometrical Model.

4.2. NLFE Ultimate Failure and First Crack Load

The ultimate and first crack loads obtained by NLFE analysis for the four groups under distributed compressive loading and the enhancement ratios are shown in table 5. The control specimen W1 in group I has a NLFE ultimate load of 577.16 KN. The enhancement ratio for group II was 4.3%, 0.32% and 10.7% for W3, W4 and W5 respectively while W2 has a negative effect on ultimate load by 1.59%. Group III specimens W6, W7 and W8 showed enhancement ratio in NLFE ultimate load by 5.16%, 4.58% and 12.83% respectively. The enhancement ratio for group IV specimen (W9) was 10.09%.

Table 5. All Specimens NLFE Ultimate and First crack Loads and Enhancement Ratios.

Groups	Specimen ID.	NLFEA Loads		Enhancement ratio $\left(\frac{P - P\,control}{P\,control} \times 100\right)$	
		F.C.L KN	Ultimate Load KN	F.C.L	Ultimate Load
Group I	W 1	290.00	577.16	----	----
Group II	W 2	290.00	568.00	0.00	-1.59
	W 3	290.00	601.99	0.00	4.30
	W 4	290.00	578.98	0.00	0.32
	W 5	290.00	638.90	0.00	10.70
Group III	W 6	290.00	606.92	0.00	5.16
	W 7	290.00	603.60	0.00	4.58
	W 8	290.00	651.21	0.00	12.83
Group IV	W 9	290.00	635.42	0.00	10.09

4.3. NLFE Crack Patterns and Modes of Failure

The cracking was initiated at early loading stage in the walls modelling about the supported edges due to compressive loading of the walls and the cracks also forms along the out of plane face of the specimens as shown in Fig. 14. Table 5 shows that regardless of the reinforcing characteristics, all the specimens had a first cracking load of 290 KN. Due to the microscopic cracks that aren't visible during the experimental testing phase, cracks have already begun at this point. Compared to the experimental first cracking loads, the NLFEA first cracking loads found to be quite lower.

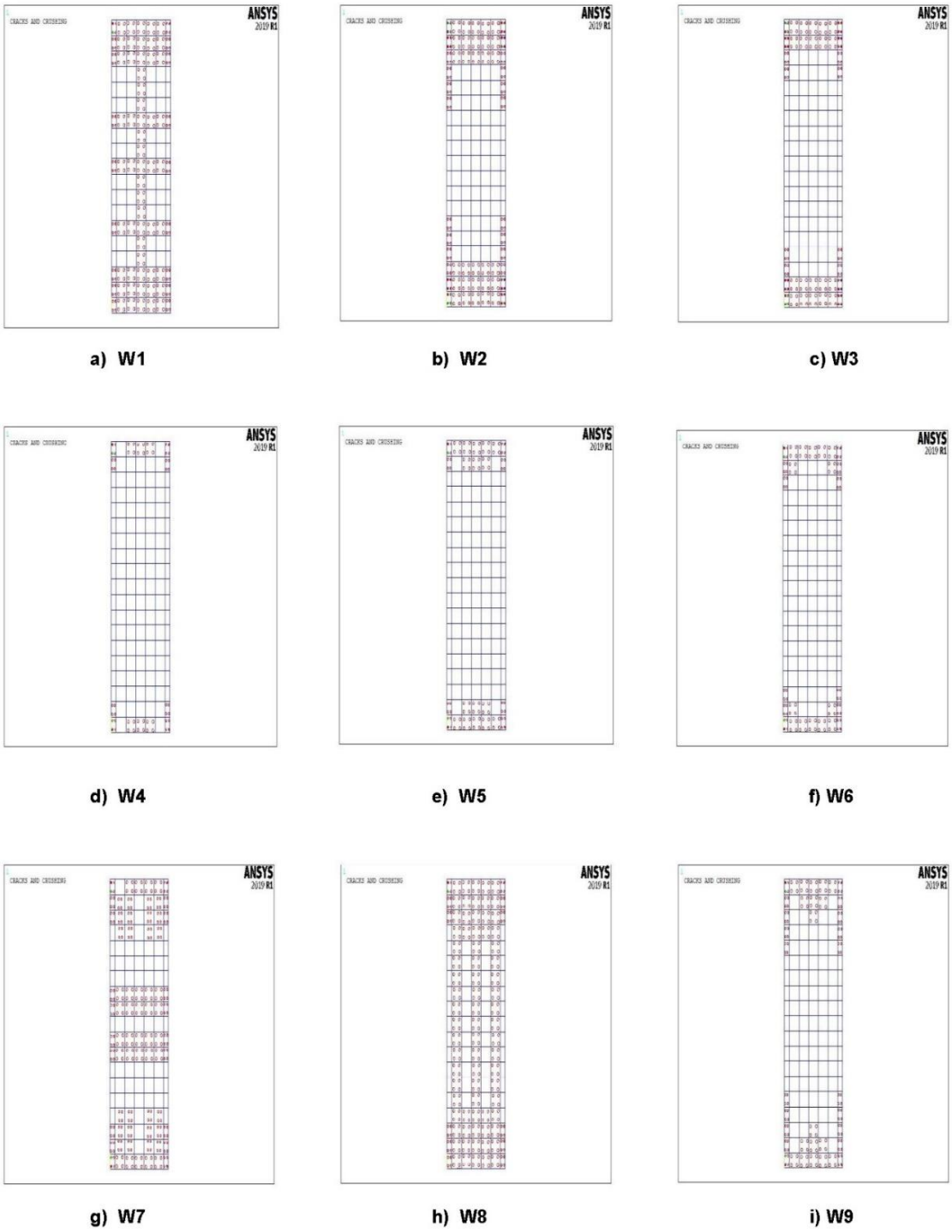

Figure 14: NLFEA Crack Patterns.

5. Comparisons Between Experimental and NLFEA Results

After applying the NLFE model, it was found that the experimental findings and the results from ANSYS 2019-R1 were in good agreement between them. Comparisons were made between the loads at which the first crack appeared, the loads at which the failure occurred, the load-vertical displacement curves, and the crack patterns.

5.1. Comparison of Experimental and NLFE Ultimate Failure and First Crack Loads

The comparisons between the obtained results for all groups are shown in Table 6. The P NLFEA/P exp. for the ultimate failure load have showed average ratio of 0.88 and The P NLFEA/P Exp. for the first crack load have showed average ratio of 0.66. A variance of 0.006 and 0.0004 and standard deviation of 0.0247 and 0.0207 for the ultimate and the first crack loads respectively. Figure 15 compares the ultimate failure load determined experimentally with that determined by the NLFEA, and Figures 16 and 17 compare the load-vertical displacement curves determined experimentally and by the NLFEA for all groups. The load-vertical displacement of the NLFEA model have shown semi-identically with the experimental curves. This similarity showed that the NLFEA model could give a great prediction of the mechanical properties for the ferrocement walls.

5.2. Comparison of Experimental and NLFE Cracks and Modes of Failure

Initial cracks showed to occur on the edges of the specimens in both experimental and NLFEA model, and these cracks propagated vertically on specimens, while additional flexural cracks formed when the strain of the specimens was increased. In both cases, when the applied force reached the point of failure, the specimens cracked diagonally. The NLFEA model showed a good agreement and similarity in the crack patterns for all specimens as shown in a sample of the experimental and NLFE cracked walls in Fig. 18. This similarity in crack patterns promotes the use of the NLFEA model in future studying different properties of ferrocement elements.

Table 6. Comparisons Between Experimental and NLFEA Results.

Groups	Specimen ID.	Experimental Loads		NLFEA Loads		$\left(\frac{P\ (NLFEA)}{P\ (Exp.)}\right)$	
		F.C.L KN	Ultimate Load KN	F.C.L KN	Ultimate Load KN	F.C.L	Ultimate Load
Group I	W 1	425.64	655.87	290.00	577.16	0.68	0.88
Group II	W 2	428.48	668.24	290.00	568.00	0.68	0.85
	W 3	430.65	676.40	290.00	601.99	0.67	0.89
	W 4	432.22	681.16	290.00	578.98	0.67	0.85
	W 5	451.44	717.87	290.00	638.90	0.64	0.89
Group III	W 6	430.58	674.36	290.00	606.92	0.67	0.90
	W 7	434.21	685.91	290.00	603.60	0.67	0.88
	W 8	470.56	766.13	290.00	651.21	0.62	0.85
Group IV	W 9	436.39	690.67	290.00	635.42	0.66	0.92
Average						0.66	0.88
Variance						0.0004	0.0006
Standrad Deviation						0.0207	0.0247

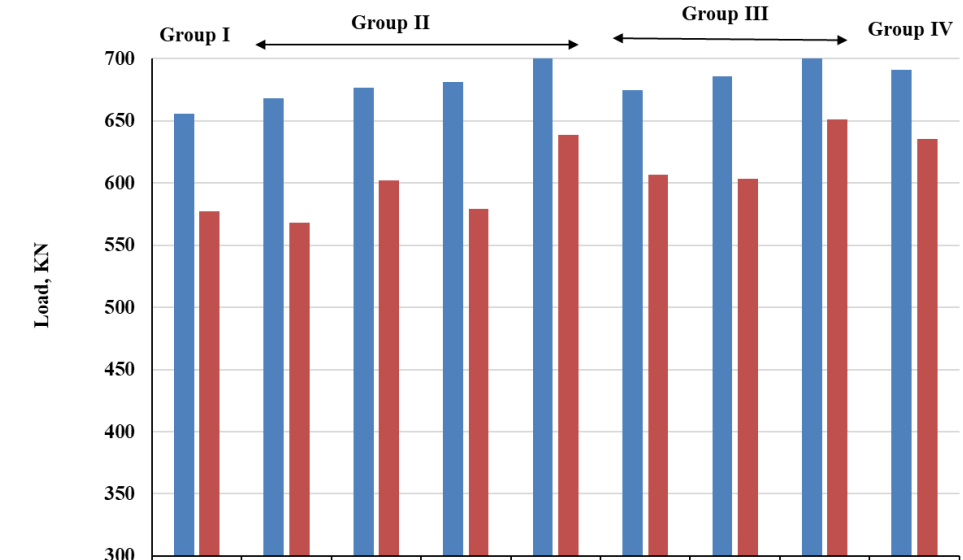

	W1	W2	W3	W4	W5	W6	W7	W8	W9
P.ult.Exp. KN	655.87	668.24	676.40	681.16	717.87	674.36	685.91	766.13	690.67
P.ult.NLFEA KN	577.16	568.00	601.99	578.98	638.90	606.92	603.60	651.21	635.42

Figure 15: Experimental and NLFE Ultimate Failure Loads Comparison.

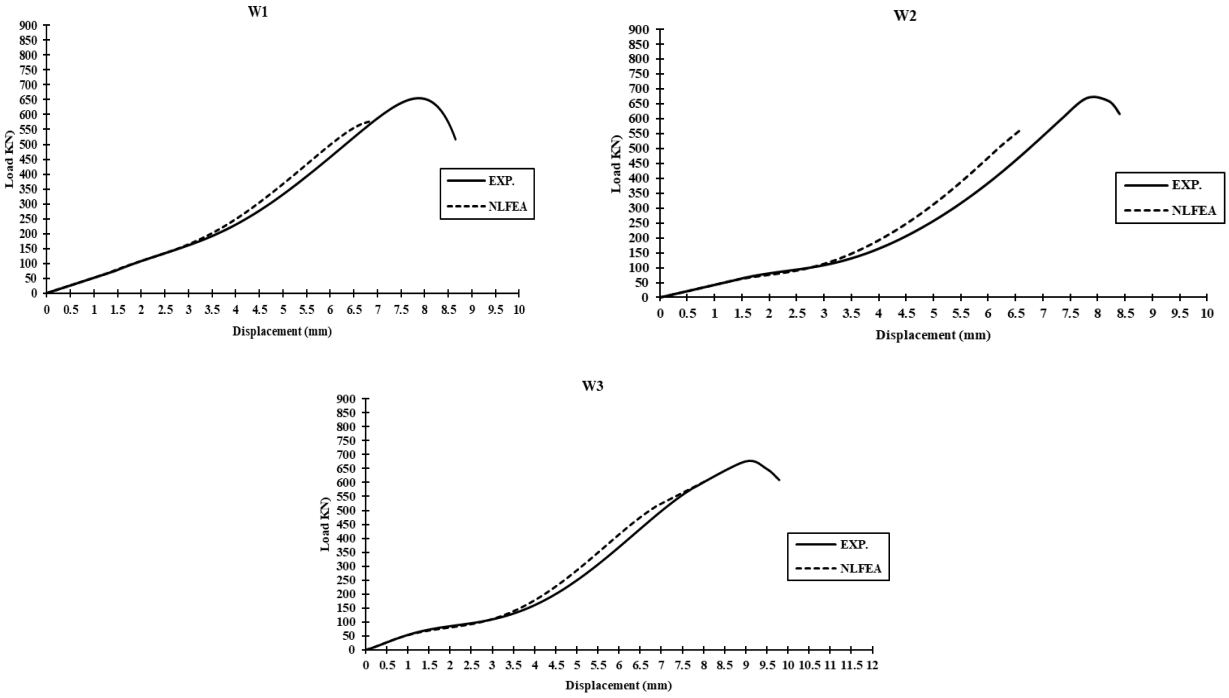

Figure 16: NLFEA Vs. Experimental Load-Vertical Displacement Curves (W1: W3).

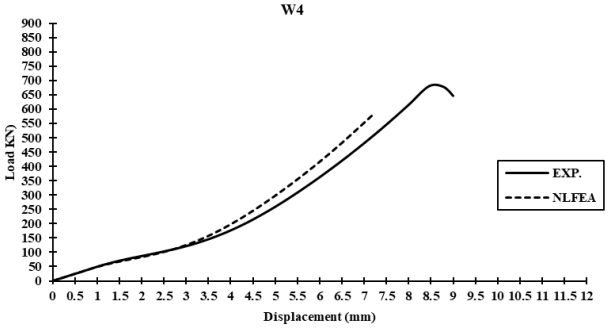

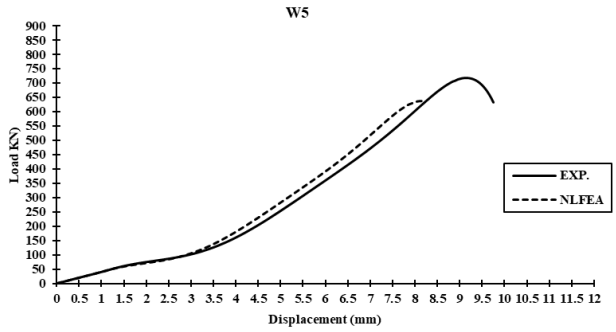

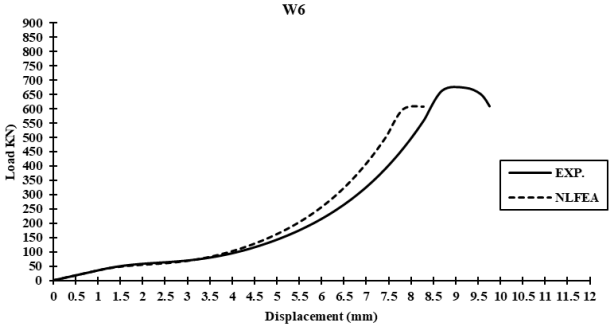

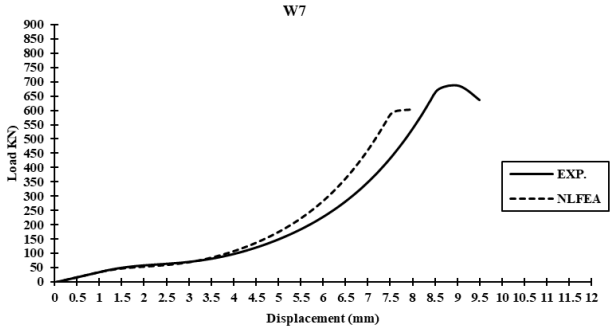

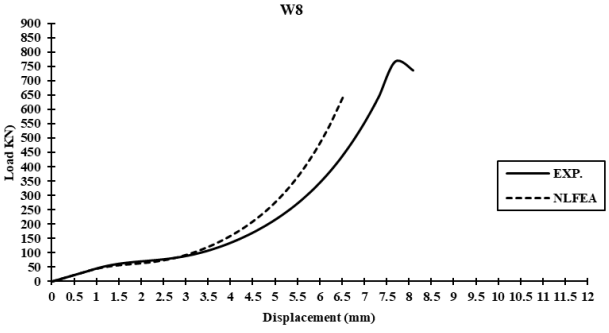

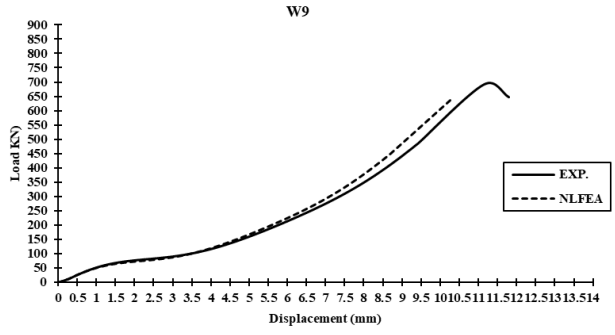

Fig.17 NLFEA Vs. Experimental Load-Vertical Displacement Curves (W4: W9).

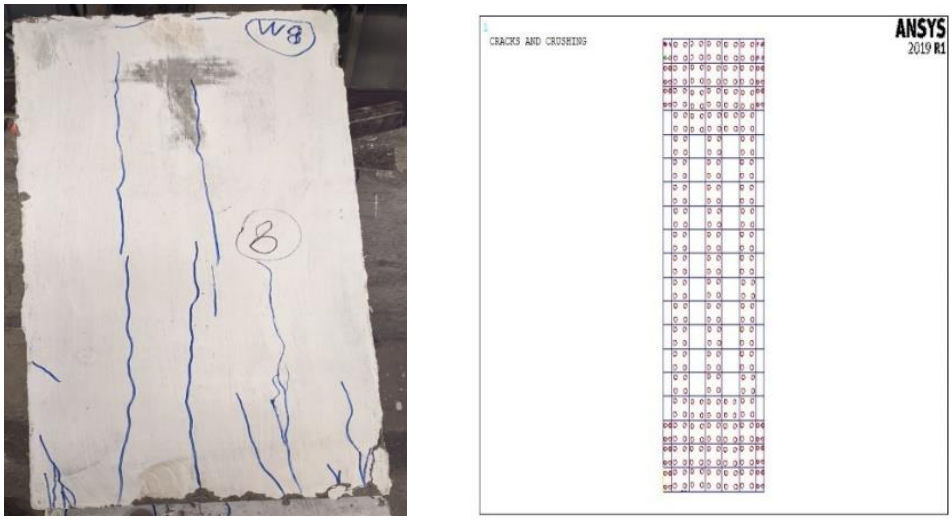

a) **b)**

Figure 18: Experimental and NLFE Crack Patterns of Specimen W8 Comparison; a) Experimental; b) NLFE

6. Conclusions

To investigate the structural efficiency of the ferrocement light walls, an experimental program was developed and conducted. The present work presents and discusses the results of a distributed compressive loading tests conducted on nine walls divided into four groups, included observations and calculations of the first crack loads, service. Loads, ultimate failure load, ductility ratios, energy absorption, the relations between load and vertical displacement, the load-horizontal displacement curves, and the crack patterns. A NLFEA simulation model using ANSYS 2019-R1 was also used to compare the results of NLFEA model with the experimental results and to evaluate the efficiency of the NLFEA model. This study presents the results and observations from the experimental and the analytical investigation, from which the following conclusions can be drawn:

1) The results of the Compressive load testing of all the walls showed that adding ferrocement provided a higher ultimate load and strength increase than using traditional reinforced concrete only.
2) The ultimate loads of ferrocement specimens examined with distributed compression loadings are higher than those of control specimen by average ratio of 5.98%, regardless of whether the steel reinforcement is expanded or welded.
3) The ultimate loads under distributed compression loading are greatly influenced by the different types of steel mesh, whether expanded or welded. Strength is improved in expanded steel mesh-reinforced samples compared to welded steel mesh- reinforced

samples with average ratios of 8.07% for the expanded mesh-reinforced samples to 4.58% for the welded mesh-reinforced samples.

4) The specimens with welded steel mesh layers gave superior mechanical properties better than the control specimen noting that the welded mesh have smaller diameter and lighter in weight than the expanded mesh.
5) The wall W8 which have 3 expanded steel mesh layers have the highest ultimate failure load of 766.13 KN, first crack load of 470.56 KN and service. Load of 478.18 KN and the highest ductility ratio of 5.09 and energy absorption of 1922.34 KN.mm compared to all specimens.
6) The use of steel meshes have a negative effect on energy absorption by average ratio of -18.55% except in the walls W5, W8 and W9 which have better energy absorption than the control wall by average ratio of 14.13%.
7) Using a mix of welded and expanded steel mesh layers like in wall W9 enhances the mechanical properties and cracking control of the specimen.
8) The mechanical behavior of ferrocement lightweight walls could be studied using a finite element model, with the results agreeing well with the existing data from full- scale tests with approximately ratio of 88%.

References

[1] Fahmy, E., and Shaheen, Y. "Laminated ferrocement for strengthening and repairing of reinforced concrete beams". Proceedings of the Annual Conference of the Canadian Society for Civil Engineering, 475-483., 1994.

[2] Fahmy, E.H., Shaheen, Y.B.I, and Korany, YS. "Repairing Reinforced Concrete Columns Using Ferrocement Laminates", Journal of ferrocement, 29, No.2, 115-124, 1999.

[3] Swamy, R.N. and Spanos, "Deflection and cracking Behavior of Ferrocement with Grouped Reinforcement and Fiber Reinforced Matrix". ACI Journal 79-91, 1988.

[4] Fahmy, E. H., Shaheen, Y. B., Abou Zeid, M. N., & Gaafar, H. (2004, August). Ferrocement sandwich and cored panels for floor and wall construction. In Proceedings of the 29th Conference on our World in Concrete & Structures (pp. 245-252).

[5] ACI Committee 549 (1997) State-of-the-Art report on ferrocement. ACI549-R97, in manual of concrete practice. ACI, Detroit, p 26.

[6] Shaheen, Y. B., Mousa, M., & Gamal, E. E. (2020, December). Structural behavior of light weight ferrocement walls. In IOP Conference Series: Materials Science and Engineering (Vol. 974, No. 1, p. 012037). IOP Publishing.

[7] Fahmy, E. H., Shaheen, Y. B., Abdelnaby, A. M., & Abou Zeid, M. N. (2014). Applying the ferrocement concept in construction of concrete beams incorporating reinforced mortar permanent forms. International Journal of Concrete Structures and Materials, 8(1), 83-97.